Available online at www.sciencedirect.com

SciVerse ScienceDirect

Ceramics International 39 (2013) 7767–7772

CERAMICS INTERNATIONAL

www.elsevier.com/locate/ceramint

Structural investigation of boron undoped and doped indium stabilized bismuth oxide nanoceramic powders

Serhat Koçyiğit[a], Özge Gökmen[b], Sinan Temel[b], Arda Aytimur[a], İbrahim Uslu[a], Sevgi Haman Bayari[c,*]

[a]Gazi University, Faculty of Education, Department of Chemistry Education, 06500 Ankara, Turkey
[b]Bilecik Şeyh Edebali University, Central Laboratory, 11210 Gülümbe/Bilecik, Turkey
[c]Hacettepe Universities, Faculty of Education, Department of Physics, 06800 Ankara, Turkey

Received 25 January 2013; received in revised form 11 March 2013; accepted 12 March 2013
Available online 21 March 2013

Abstract

The synthesis of boron undoped and doped indium stabilized bismuth oxide nanoceramic powders via the polymeric precursor technique were described. The physical properties of the precursor polymer solutions (pH, surface tension, viscosity and conductivity) were measured.

The morphological and structural characteristics of the nanoceramic powders were investigated by X-ray diffraction (XRD), Scanning Electron Microscopy (SEM) and Fourier transform infrared spectroscopy (FTIR).

The lattice constant, average particle size, microstrain and dislocation density of the samples were calculated. The results show that the average particle size decreased while both the microstrain and the dislocation density values increased in the boron doped indium stabilized bismuth oxide. The structure proposed from FTIR spectra is mainly based on BiO_6 and BiO_3 units.

Keywords: Bismuth oxide; Indium; Boron doped; Nanoceramic powders

1. Introduction

Nanocrystalline materials have attracted much attention, because of their specific properties in optical, electronic, magnetic and mechanical applications [1].

Bismuth oxide based materials exhibit high oxide ionic conductivity and has been proposed as good electrolyte materials for applications, such as solid oxide fuel cells (SOFC) and oxygen sensors [2–4]. Solid oxide fuel cells are viewed as important to the future of greener and more efficient energy sources.

Bismuth oxide (Bi_2O_3) exists as five crystallographic polymorphs (monoclinic α-phase, tetragonal β-phase, body centered cubic γ-phase (bcc), face centered cubic δ-phase (fcc) and triclinic) [5,6]. The monoclinic α-phase and γ-bcc forms are semiconductors, whereas the β-tetragonal and δ-fcc forms are oxide ion conductors. δ-phase bismuth oxide (δ-Bi_2O_3) has a fluorite type structure and high conductive oxide ion conductor [3,7,8]. However, this phase only stable between 730–825 °C. It is possible to obtain at room temperature by doping with some transition metal and rare earth metal ions and oxides [9,10].

δ-Bi_2O_3 can be stabilized down to room temperature by the additions of indium oxide (In_2O_3). In_2O_3 in the bulk form has been widely used in solar cells and organic light emitting diodes [11,12]. Indium stabilized δ-Bi_2O_3 can be synthesized by various techniques including mechanochemical synthesis, powder milling and mixing and the polymeric precursor technique (PPT). The PPT appears the most attractive for the preparation of cubic δ-Bi_2O_3 based ionic conductors which employs of complexing of metal acetate/nitrate precursor in a polymer solution for example PVA. The main advantage of polymeric precursor technique is the homogeneity of the precursors on a molecular level.

Boron oxide, B_2O_3 formed by the thermal fusion of boric acid (H_3BO_3). It has amorphous form and is an excellent

*Corresponding author. Tel.: +90 312 2978606; fax: +90 312 2978600.
E-mail addresses: bayari@hacettepe.edu.tr, bayarisevgia@gmail.com (S. Haman Bayari).

0272-8842/$ - see front matter © 2013 Elsevier Ltd and Techna Group S.r.l. All rights reserved.
http://dx.doi.org/10.1016/j.ceramint.2013.03.035

network former. Boron oxides have the advantage of low heat expansion and high refractive index. Because of these natures, boron oxides are used widely in glass ceramics composition. According to previous experimental results [9,13–15], the addition of boron oxide to the bismuth oxide is very beneficial and it is very effective as a sintering aid. It reduced the processing temperature because of its low melting point and could help resulting in smaller grain sizes and grain boundary strengthening during the calcination stage.

The purpose of the present study was to investigate of boron doped and undoped indium stabilized bismuth oxide nanoceramic powders in order to establish the structural changes induced by indium and boron to the bismuth oxide. Nanoceramic powders were obtained by the calcination method to remove of the organic phase from precursor polymer solution.

The physical properties of solutions such as pH, surface tension, viscosity, and conductivity were measured. The structures of boron doped and undoped indium stabilized bismuth oxide nanoceramic powders were investigated by X-Ray diffraction (XRD), FTIR spectroscopy and Scanning Electron Microscope (SEM).

2. Experimental section

2.1. Materials and method

In the experiment, bismuth (III) acetate (99 · 99%, Aldrich), indium acetate (99 · 99%, Aldrich) and polyvinyl alcohol (PVA) (Aldrich, molecular weight=85,000–124,000) were used as starting materials and ultrapure deionized water was used as a solvent. Boric acid was obtained from Merck and ultrapure deionized water was used as a solvent. The experimental procedure is schematically shown in Fig. 1.

Aqueous PVA solution (10%) was first prepared by dissolving PVA powder in distilled water and heating at 80 °C with stirring for 2 h, then cooling to room temperature. Then, 1.5 g of bismuth(III) acetate and 0.3781 g of indium acetate were added to the 30 g aqueous PVA at 60 °C separately and the solution was vigorously stirred for 1 h at this temperature. Stirring was continued for 3 h at room temperature. Thus, viscous gels of PVA/Bi-In acetate hybrid polymer solution (solution In1) were obtained. Boron doped solution (solution In2) was prepared using the same procedure of solution In1 and adding 0.25 g of the boric acid. Finally, the boron undoped and doped hybrid polymer solutions were calcined at a rate of 8 °C/min for 2 h at 850 °C at atmospheric conditions. The resulting oxide nanoceramic powders obtained from solutions were ground into powder using a mortar.

2.2. Measurement and characterization

The pH and conductivity of the polymer solutions were measured using pH 315i meter (Wissenschaftlich-Technische Werkstätten (WTW) GmbH & Co. KG) and conductivity meter (Wissenschaftlich-Technische Werkstätten (WTW) GmbH & Co. KG), respectively. The viscosity of the solutions was determined using a SV-10 viscometer. Surface tension measurements were performed using a KRUSS manual measuring system.

X-ray powder diffraction patterns of nanoceramic powders were collected using a PANalytical Empyrean X-Ray diffractometer using Cu Kα radiation ($\lambda = 1.54$ Å).

The surface morphology of nanoceramic powders was examined by using Field Emission Scanning Electron Microscopy (FESEM-Carl Zeiss, Supra 40 VP) with an accelerating voltage of 10 kV. The samples were sputter-coated with platinum (Qourum Q 150 R ES DC Sputter). ImageJ-Image-Pro

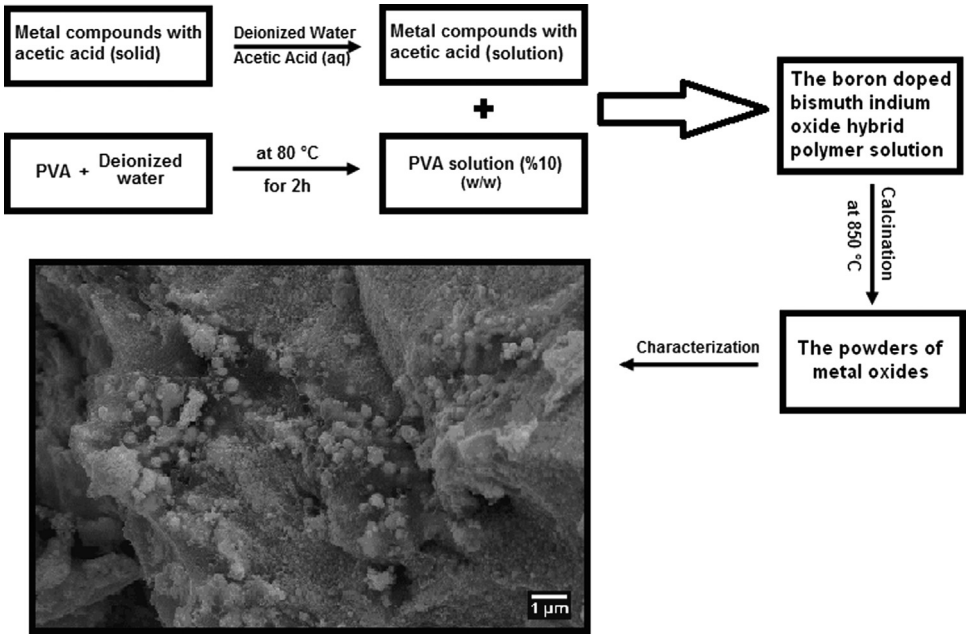

Fig. 1. Schematic of experimental procedure for synthesizing nanoceramic powders.

Express (Version 5.0.1.26) software was usedin order to obtain the particle diameter.

FTIR spectra (4000–400 cm^{-1}) were recorded on a Perkin-Elmer Spectrum 100 FTIR spectrometer from KBr pellets and by ATR (with a diamond protected attenuated total reflectance crystal unit) at a resolution of 4 cm^{-1}after 100 scans.

3. Results and discussion

3.1. Physical Properties of the polymer solution

The results of pH, density and surface tension of In1 and In2 are depicted in Table 1.

There were no significant differences in surface-tension values (Table 1). It appears that the surface tension value is not dependent the addition of boric acid.

On the other hand, the pH and viscosity values between two samples were noted to be significantly different.

δ-Bi_2O_3 has a conductivity of-~1 mho cm^{-1} = 1 S cm^{-1} at 730 °C and the conductivity in the β-phase is predominantly ionic with oxide ions being the main charge carrier. The conductivity as a function of dopant type and temperature has been studied widely [9,16–19]. The cubic fluorite structure can be stabilized by the addition of the metal ions but the conductivity drops by over two orders of magnitude.

In this study, we also aimed more information about conductivity properties of solutions. The addition of boric acid as boron source as a crosslinking agent increased the conductivity of the hybrid polymer solution as expected.

In comparison with some Bi-containing phases, the conductivity of boron doped and undoped PVA/Bi–In acetate solutions were higher than the electrical conductivity of boron doped and undoped PVA/Bi–gadolina acetate nanofibers [20].

3.2. X-ray diffraction and Scanning electron microscopy

The XRD patterns of the calcined boron undoped (In1) and doped (In2) indium stabilized bismuth oxide nanoceramic powders are shown in Fig. 2.

XRD patterns present several clear individual peaks, whose attribution to corresponding δ-phase bismuth oxide was identified by comparison with the data from the literature. All peaks are assigned to the δ-Bi_2O_3 phase in agreement with the result given by JCPDS (78-2027). As can be seen from the Fig. 2 (a), the highest peak, from $2\theta = 28.18^\circ$ (111) to related to the face-centered cubic unit cell of δ-Bi_2O_3.Three peaks at 2θ values of 32.96°, 46.49°, and 54.50° corresponding to (002), (022), and (113) planes of δ-Bi_2O_3 powders were observed in the undoped indium stabilized bismuth oxide (In1).

The XRD pattern of boron doped indium stabilized bismuth oxide (In2) is shown in Fig. 2(b).

In this case, the Bi_2O_3 exhibit the cubic phase with characteristic 2θ values at 28.22°, 32.86°, 46.33°, 54.40°. The intensity of the peaks is lower than boron doped indium stabilized bismuth oxide.

A decrease of the Bi_2O_3 (111) peak intensity with boron doped produces lower crystallinity for boron doped In2 sample (Fig. 2(b)). This finding suggests that the incorporation of boron atoms into the In2 prevents the nucleus formation and turns the structure into a more glassy form.

The structural parameters (the lattice constant, the crystallite dimension, dislocation density and microstrain) for the boron undoped (In1) and doped (In2) samples were calculated by using relevant equations and are presented in the Table 2.

The lattice constant (a) is determined by comparing the peak positions (2θ) of the XRD pattern of the In1 sample with that of In2 using the Eq. 1. [21]

$$\frac{1}{d^2} = \frac{h^2+k^2+l^2}{a^2} \quad (1)$$

The calculated lattice constants (a) of the undoped indium stabilized bismuth oxide nanoceramic powders were found to agree well with the values in our previous results [9,14].

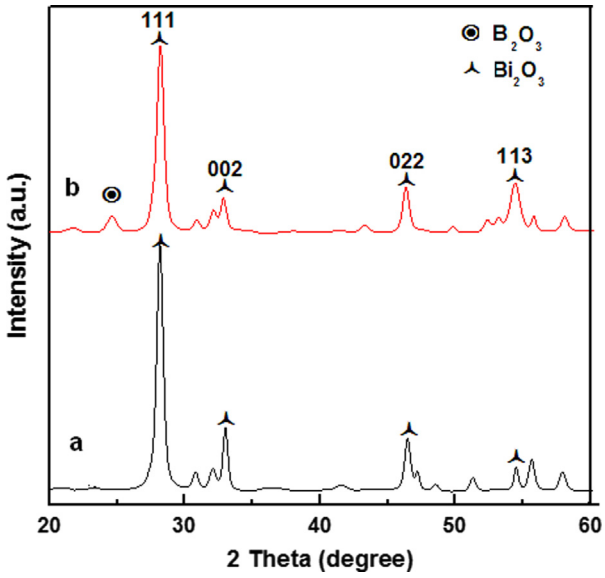

Fig. 2. The X-ray diffraction patterns of the crystalline structure of calcined boron undoped (a) and doped (b) indium stabilized bismuth oxide nanoceramic powders.

Table 1
Physical properties of the polymer solutions.

Solution	pH	Electrical conductivity (mS/cm)	Viscosity (mPas)	Surface tension (mN/m)
In1	2.56	1.53	88.4	52
In2	2.48	1.56	122	53

Table 2
Calculated structural parameters of the calcined nanoceramic powders.

Sample	(*hkl*)	2*θ* (°)	FWHM (°)	*d* (Å)	*a* (Å)	*D*(nm)	$\delta \times 10^{-11}$(cm^{-2})	$\varepsilon \times 10^{-3}$
In-1	(111)	28.18	0.5774	3.1641	5.4803	14.2	4.9697	4.4611
	(002)	32.96	0.4349	2.7153				
	(022)	46.49	0.5055	1.9517				
	(113)	54.50	0.3531	1.6823				
In-2	(111)	28.22	0.6427	3.1597	5.4727	12.7	6.1563	4.9583
	(002)	32.86	0.5496	2.7233				
	(022)	46.33	0.5459	1.9581				
	(113)	54.40	0.7548	1.6852				

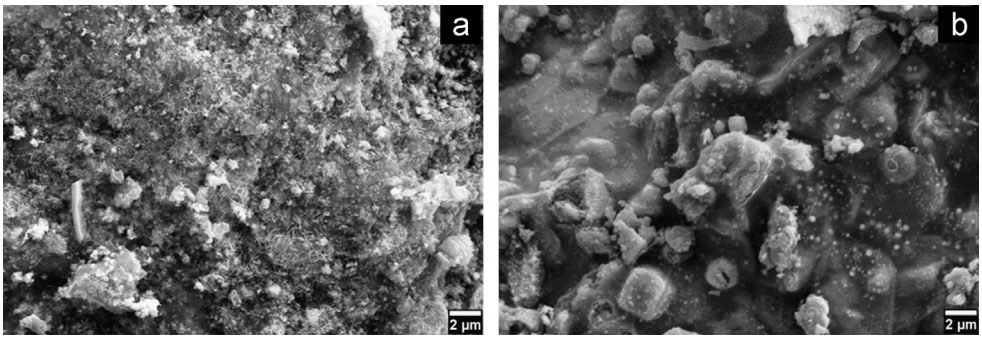

Fig. 3. SEM images of the the boron undoped(a) and doped (b) In-Bi oxide nanoceramic powders.

Studies of materials in the nanoscale need characterization of microstructure with emphasis in the particle size and microstrain. To estimate the particle size using X-ray powder diffraction (XRD) measurements, the Scherrer equation is the most used method [22,23].

The crystallite dimension (D_{hkl}) or average particle size of the boron doped indium stabilized bismuth oxide nanoceramic powders was calculated for the preferred planes [*h*,*k*,*l*] by the X-ray line broadening method using the Scherrer equation,

$$D_{hkl} = \frac{k\lambda}{\beta_{hkl} cos\theta} \tag{2}$$

where, k=0.9 (Scherrer constant), λ is the wavelength of the X-ray radiation used (0.15405 nm), θ is the Bragg angle for the crystal planes {*hkl*}, and β_{hkl} is the full-width at half-maximum (FWHM)) intensity of the peak for which the particle size is to be calculated and θ is the Bragg angle.

Dislocations are an imperfection in a crystal associated with misregistry of the lattice in one part of the crystal with respect to another part. The dislocation density (δ) and the microstrain (ε) of the boron doped/undoped indium stabilized bismuth oxide nanoceramic powders were also calculated by the Eqs. 3 and 4.

$$\delta = \frac{n}{D^2} \tag{3}$$

where n is a factor (n=1 for minimum dislocation density) [24].

$$\varepsilon = \frac{1}{tan\,\theta}\left(\frac{\lambda}{Dcos\,\theta} - \beta_{hkl}\right) \tag{4}$$

The X-ray diffraction peaks were broadened in boron doped sample due to small grain size. The average particle size of the boron doped In2 sample was smaller than that of the undoped In1 sample. The microstrain and the dislocation density values were found to increase after boron doped (Table 2).

The boron may cause a decrease in crystallite size and transition to the amorphous glassy structure which is consistent with literature [25]. Reduction of grain size to the nano-scale leads to improvements by increasing the number of atoms in the grain boundary [26,27].

The SEM images of the boron undoped and doped In-Bi oxide nanoceramic powders are shown in Fig. 3(a) and (b), respectively. Boron undoped (In1) structure consists of some needle-like crystals (Fig. 3 (a)). It can be seen from Fig. 3 (a) the size of the of the needle-like crystals is about 10 nm width and length up to 500 nm. Boron behaves as glassy network former and the incorporation of B_2O_3 atoms into the indium stabilized Bi_2O_3 turns the structure into a more glassy form as seen from Fig. 3 (b). These observations are consistent with results of XRD (Fig. 2).

3.3. FTIR spectra

The molecular structure of the boron undoped (In1) and doped (In2) indium stabilized bismuth oxide nanoceramic powders were also analyzed by FTIR spectroscopy. FTIR spectra of the samples are presented in Fig. 4. For comparison purposes Fig. 4 also includes infrared spectra of poly(vinyl alcohol) [$(C_2H_4O)_n$], bismuth acetate [$Bi(CH_3CO_2)_3$], indium

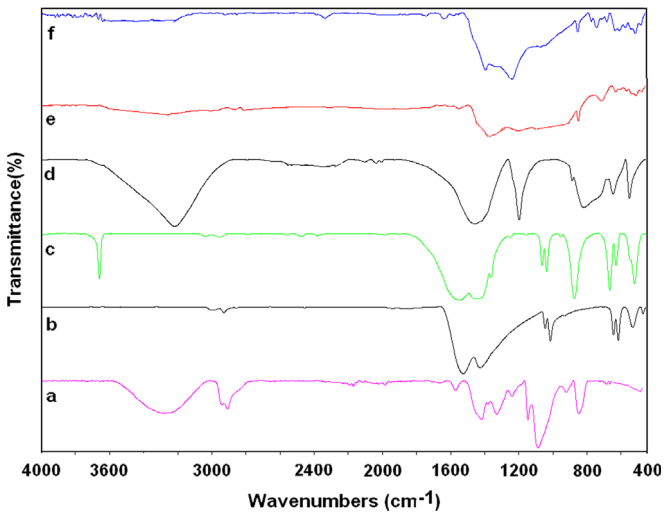

Fig. 4. FTIR spectra of various samples: (a) PVA (b) Bismuth acetate (c) Indium acetate (d) boric acid (e) calcined boron undoped Bi-In nanoceramic powders and (f) calcined boron doped Bi-In nanoceramic powders.

acetate, $[In(CH_3CO_2)_3]$ and boric acid $[B(OH)_3]$ used in experiments. The observed wave numbers and proposed assignments are summarized in Table 3 for PVA, bismuth acetate, indium acetate, boric acid, In1 and In2 nanopowders. FTIR data of In1 and In2 were discussed by comparing the experimental data of related compounds.

It is known that the infrared spectrum of the monoclinic α-phase Bi_2O_3 presents seven bands at 670, 620, 595 545 510, 465, and 425 cm^{-1} in the 400–600 cm^{-1} region [28,29]. These bands are related to the vibrations of Bi-O bonds in BiO_6 octahedral units.

The infrared spectrum of Bi_2O_3 also presents five infrared bands at 470, 540,620 and 840 cm^{-1} characteristic of the vibrations of Bi-O bonds in BiO_3 pyramidal units. The bands at 707 cm^{-1} and 732 cm^{-1} are related to the stretching vibrations of Bi–O in BiO_3 units [30].

The infrared absorption bands for Boron oxide were assigned with spectra published in the on literature [31–33].

As can be seen from Fig. 4, organic molecules are removed completely from calcined nanoceramic powders. Vibrational spectra of Bi_2O_3 and derivatives studied by infrared spectroscopy indicated that bismuth does not form a simple structure. However, it is well known that bismuth ions can form $[BiO_3]$ pyramidal or $[BiO_6]$ octahedral units. The observed bands in the infrared spectra of In1 and In2 confirm the formation of Bi_2O_3 and the structure proposed from FTIR spectra of In1 and In2 samples is mainly based on BiO_6 and BiO_3 units. These results are consistent with the findings of the previous studies on the stabilized bismuth oxide nanopowders [19]. The shape and the intensity of the bands in In2 are changing, which can be due to the contribution of the vibrations of B–O bonds.

4. Conclusions

Boron undoped and doped indium stabilized bismuth oxide nanoceramic powders were synthesized using polymeric

Table 3
Observed wavenumbers (cm^{-1}) and assignments for the studied samples [aa].

PVA		Bismuth acetate		Indium acetate		Boric acid [a]		In1		In2	
IR	Assign.	IR	Assign.	IR	Assign.	IR	Assign.	IR	Assign.	IE	Assign.
3245	ν(OH)			3655		3216	ν(OH)				
2900–2950	$\nu(CH_2)$	3005–3020	$\nu(CH_3)$	3040–2950	$\nu(CH_3)$						
1646,1560	ν(CC)	1520	CO	1543	CO						
1412	$\delta(CH_2)$	1418	$\delta(CH_3)$	1439	$\delta(CH_3)$	1455	ν(B-O)	1389	Bi-O in BiO_6	1384	ν(B–O) in BO_2O^-
1372	$\delta\ (CH_2)$	1042	$\rho(CH_3)+\ \nu$ (C-O)	1359	$\delta(CH_3)$	1193	δ(B-O-H)			1230	B–O bonds in BO_3 units
1320	δ(CH+OH)	1011	$\rho(CH_3)$	1058	ν (C-O)	884	ν (B-O)				
1235	ν(C–O–C)+CH			1031	$\rho(CH_3)$	813	δ(B-O-H)	846	ν(Bi-O).in BiO_3	845	ν(Bi -O).in BiO_3
1142	crystallization-sensitive band			949	ν(CC)	675		707	ν(Bi–O) in BiO_3 unit	763	O_3B–O–BO_4 linkage
1083	ν (C-O)			869		667				734	ν(Bi- O) in BiO_3
911	$\nu(CC)+\ \rho(CH_2)$	640	δ (O-C-O)	662	δ (O-C-O)	642	δ BO_3			675	Bi –O bonds in BiO_6 or B–O–B linkage in the borate network
840	$(CH_2)+\nu(CC)$	611	δ (C=O)	627	γO-C-O						
		526	γ(C=O)	617	γO-C-O	546	δ(OBO)	505	δ(Bi – O) in BiO_6	505	δ(Bi – O) in BiO_6
		465	ν(Bi-O)	516				471	δ(Bi – O) in BiO_3	472	δ(Bi – O) in BiO_3

[aa]Vibrational modes: ν, stretching; δ, in-plane bending,γ, out-of-plane bending, ρ rocking.
[a]Taken from Ref [32].

precursor technique. The viscosity and pH values are increased and decreased, respectively by addition of boron in solution. The electric conductivity is also increased in boron doped sample. X-ray Diffraction analysis showed that the calcined nanopowders have stable cubic δ-phase (fcc) Bi_2O_3 which was also supported by the FTIR The added boron to the bismuth oxide promote a decrease in grain size.

References

[1] C. Suryanarayana, C.C. Koch, Nanocrystalline materials—current research and future directions, Hyperfine Interactions 130 (2000) 5–44.

[2] T. Takahashi, H. Iwahara, T. Esaka, High oxide ion conduction in sintered oxide of the system Bi_2O_3–M_2O_3, Journal of the Electrochemical Society 124 (1977) 1563–1569.

[3] N.M. Sammes, G.A. Tompsett, H. Nafe, F. Aldinger, Bismuth based oxide electrolytes structure and ionic conductivity, Journal of European Ceramic Society 19 (1999) 1801–1826.

[4] N. Jiang, E.D. Wachsman, S.H. Jung, A higher conductivity Bi_2O_3-based electrolyte, Solid State Ionics 150 (2002) 347–353.

[5] B. Aurivillius, L.G. Sillen, Polymorphy of bismuth trioxide, Nature 155 (1945) 305–306.

[6] H.A. Harwig, On the structure of Bismuthsesquioxide: the α, β, γ, and δ-phase, Zeitschrift für anorganische und allgemeine Chemie 444 (1978) 151–166.

[7] H.A. Harwig, J.W. Weenk, Phase relations in bismuthsesquioxide, Zeitschrift für anorganische und allgemeine Chemie 444 (1978) 166–177.

[8] V.V. Kharton, E.N. Naumovich, A.A. Yaremchenko, F.M.B. Marques, Research on the electrochemistry of oxygen ion conductors in the former Soviet Union: IV. Bismuth oxide based ceramics, Journal of Solid State Electrochemistry 5 (2001) 160–187.

[9] A. Aytimur, S. Kocyigit, I. Uslu, S. Durmusoglu, A. Akdemir, Fabrication and characterization of bismuth oxide-holmia nanofibers and nanoceramics, Current Applied Physics 13 (2013) 581–586.

[10] M. Arı, S. Tascioglu, A. Altindal, I. Uslu, T. Karaaslan, S. Kocyigit, Crystal structure and electric properties of gadolinia doped bismuth oxide nanoceramic powders, Materials Chemistry and Physics 136 (2012) 942–946.

[11] K. Sreenivas, T.S. Rao, A. Mansingh, S. Chandra, Preparation and characterization of Rf sputtered indium tin oxide films, Journal of Applied Physics 57 (1985) 384–392.

[12] Y. Shigesato, S. Takaki, T. Haranoh, Electrical and structural properties of low resistivity of low resistivity tin-doped indium oxide films, Journal of Applied Physics 71 (1992) 3356–3364.

[13] Z.W. Zhang, C.T. Liu, S. Guo, J.L. Cheng, G. Chen, T. Fujita, M. W. Chen, Y.W. Chung, S. Vaynman, M.E. Fine, B.A. Chin, Boron effects on the ductility of a nano-cluster-strengthened ferritic steel, Materials Science and Engineering A-Structural Materials Properties Microstructure and Processing 528 (2011) 855–859.

[14] S. Durmusoglu, I. Uslu, T. Tunc, S. Keskin, A. Aytimur, A. Akdemir, Synthesis and characterization of boron-doped Bi_2O_3–La_2O_3 fiber derived nanocomposite precursor, Journal of Polymer Research 18 (2011) 1999–2004.

[15] A. Aytimur, I. Uslu, E. Cınar, S. Kocyigit, F. Ozcan, A. Akdemir, Synthesis and characterization of boron doped bismuth–calcium–cobalt oxide nanoceramic powders via polymeric precursor technique, Ceramics International 39 (2013) 911–916.

[16] R. Punn, A.M. Feteira, D.C. Sinclair, C. Greaves, Enhanced oxide ion conductivity in stabilized δ-Bi_2O_3, Journal of the American Chemical Society 128 (2006) 15386–15387.

[17] S. Yilmaz, O. Turkoglu, M. Ari, I. Belenli, Electrical conductivity of the ionic conductor tetragonal $(Bi_2O_3)1$-$x(Eu_2O_3)x$, Cerâmica 57 (2011) 185–192.

[18] M.G. Lazarraga, J.M. Amarilla, R.M. Rojas, J.M. Rojo, The cubic $Bi_{1.76}U_{0.12}La_{0.12}O_{3.18}$ mixed oxide: synthesis, structural characterization, thermal stability and electrical properties, Solid State Ionics 89 (2005) 179–196.

[19] P. Shuk, H.D. Wiemhofer, U. Guth, W. Gopel, M. Greenblatt, Oxide ion conducting solid electrolytes based on Bi_2O_3, Solid State Ionics 89 (1996) 179–196.

[20] T. Tunc, I. Uslu, S. Durmusoglu, S. Keskin, A. Aytimur, A. Akdemir, Preparation of gadolina stabilized bismuth oxide doped with boron via electrospinning technique, Journal of Inorganic and Organometallic Polymers and Materials 22 (2012) 105–111.

[21] C. Suryanarayana, M.G. Norton, X-Ray Diffraction: A Practical Approach, Plenum Press, New York, 1998.

[22] P. Scherrer, Bestimmung der Grösse und der inneren Struktur von Kolloidteilchen mittels Röntgenstrahlen, Nachrichten von der Königlichen Gesellschaft der Wissenschaften zu Göttingen 26 (1918) 98–100.

[23] H.P. Klug, L.E. Alexander, X-Ray Diffraction Procedures for Polycrystalline and Amorphous Materials, second ed., John Wiley & Sons, New York, 1974.

[24] B. Karunagaran, R.T.R. Kumar, D. Mangalaraj, S.K. Narayandass, G. M. Rao, Crystal Research and Technology 37 (2002) 1285–1292.

[25] D. Chen, D. Yang, Q. Wang, Z.Y. Jiang, Effects of boron doping on photocatalytic activity and microstructure of titanium dioxide nanoparticles, Industrial and Engineering Chemistry Research 45 (2006) 4110–4116.

[26] Y.J. Kang, H.J. Park, G.M. Choi, The effect of grain size on the low-temperature electrical conductivity of doped CeO_2, Solid State Ionics 179 (2008) 1602–1605.

[27] R. Li, Q. Zhen, M. Drache, A. Rubbens, C. Estournès, R.N. Vannier, Synthesis and ion conductivity of $(Bi_2O_3)_{0.75}(Dy_2O_3)_{0.25}$ ceramics with grain sizes from the nano to the micro scale, Solid State Ionics 198 (2011) 6–15.

[28] V. Dimitrov, Y. Dimitriev, A. Montenero, IR-spectra and structure of V_2O_5-GeO_2-Bi_2O_3 glasses, Journal of Non–Crystalline Solids 180 (1994) 51–57.

[29] R. Iordanova, Y. Dimitriev, V. Dimitrov, S. Kassabov, D. Klissurski, Glass formation and structure in the system MoO3-Bi2O3-Fe2O3, Journal of Non–Crystalline Solids 231 (1998) 227–233.

[30] I. Ardelan, D. Rusu, Structural investigations of some Bi_2O_3 based glasses, Journal of Optoelectronics and Advanced Materials 10 (2008) 66–73.

[31] C. Gautam, A.K. Yadav, A.K. Singh, A review on infrared spectroscopy of borate glasses with effects of different additives, ISRN Ceramics 2012 (2012) 428497.

[32] R. Zeebe, Stable boron isotope fractionation between dissolved $B(OH)_3$ and $B(OH)_4$, Geochimica et Cosmochimica Acta 69 (2005) 2753–2766.

[33] P. Pascuta, G. Borodi, E. Culea, Structural investigation of bismuth borate glass ceramics containing gadolinium ions by X-ray diffraction and FTIR spectroscopy, Journal of Materials Science—Materials in Electronics 20 (2009) 360–365.